MEASUREMENT SCIENCE REVIEW, **21**, (2021), No. 6, 205-208

sciendo

ISSN 1335-8871

MEASUREMENT SCIENCE REVIEW

Journal homepage: https://content.sciendo.com

Calibration of NMR Receiver using Spectrometer Characteristics

Peter Andris, Tomáš Dermek, Ivan Frollo

Institute of Measurement Science, Slovak Academy of Sciences, Dúbravská cesta 9, Sk-841 04 Bratislava, Slovakia, peter.andris@savba.sk

This article describes the measurement of the relation between input and output signals using two techniques: with a signal generator and with the thermal noise of a known resistance. Each of the techniques has its advantages and disadvantages. Both methods are tested and the results are compared. The input signal of the receiver is known in volts, while the output signal is in ADC (analogue-to-digital converter) units. It is the main difference versus the gain. Knowledge of the relation enables recalculation of the output signal into the input of the receiver or vice versa. It is important in some experiments. The method with the harmonic signal requires a suitable NMR spectroscopic console, generator of the harmonic signal and an attenuator, the method with the noise requires only the NMR console. It indicates that both methods are simple and cheap. The measured data are processed on a standard PC using common programs.

Keywords: Nuclear magnetic resonance, NMR, spectrometer, receiver, calibration.

1. Introduction

Reference [1] describes a new technique of the NMR receiver noise figure measurement using an NMR console. For successful data processing the receiver must be calibrated, it means the relation between input and output signals must be known. The relation has been determined using harmonic signal from a suitable signal generator. It is an example of an experiment where the receiver must be calibrated. Using an NMR receiver, the noise voltage can be rather simply measured. On the other hand, the noise voltage can be rather accurately calculated if parameters of the receiver are used in a proper theory. The basic theory of processing the noise signals is described in [2], [3]. Signal from an NMR experiment is rather small. Many authors studied the condition for a quality result of an acquisition [4], [5]. A quality coil system can solve many problems [6], [7]. If using a commercial NMR scanner, the RF coils are the only facility which can be changed [8], [9]. Experiments may be based on presentation of a new technique which solves problems independently of the scanner or it can be part of it [10]-[13]. Authors [14], [15] have analyzed operations with gradients pulses. The processing of the measured data is discussed elsewhere [16], [17].

Both techniques, with the signal generator and with the noising known resistance, are rather simple and cheap. They do not require special instrumentation or expensive material. Accuracy of the acquired results depends on accuracy of the used instruments.

2. Subject & methods

A simplified circuit diagram of the calibration with a signal generator is presented in Fig.1. Besides a generator with accurate signal values, it contains an attenuator, e.g., a variable attenuator. The investigated NMR receiver is basic equipment. Signal of generator is adjusted so that it is not truncated at the output of the receiver. A suitable parameter of the signal, e.g., magnitude of the harmonic signal, is taken off at the receiver input in, e.g., volts and at the receiver output in ADC (analogue-to-digital converter) units. The output data have the form of series of time samples. A ratio of the input signal (voltage) and output data (or vice versa) is calculated (what is suitable) and the resulting coefficient C can be utilized where necessary. It is obvious that this way of calibration is suitable mainly if the generator, the attenuator and the receiver are matched.

A simplified circuit diagram of the calibration with a known resistance is presented in Fig.2. Actually, this circuit is simpler than the previous circuit. Only a resistor with a known resistance and the investigated receiver are necessary. Noise at the output of the receiver can be described by, e.g., equation (1).

$$\sqrt{\left(\sqrt{4kTR_{g\_50}\Delta f}\,R_{in}/\left(R_{g\_50}+R_{in}\right)C\right)^2+V_{rec}^2}=V_{50} \quad (1)$$

k is the Boltzmann constant, $k = 1.38 \times 10^{-23}$ J/K

T is absolute temperature of the known resistance

DOI: 10.2478/msr-2021-0028

R_g is known resistance; e.g., $R_{g\_50} = 50$ Ohm

Δf is noise bandwidth

R_{in} is the characteristic impedance of the preamplifier

C is the calibration coefficient [ADC unit/V]

V_{rec} is RMS noise voltage of the receiver (depends on Δf) [ADC unit]

V_{50} is RMS noise voltage at the output of the receiver (depends on Δf) [ADC unit]

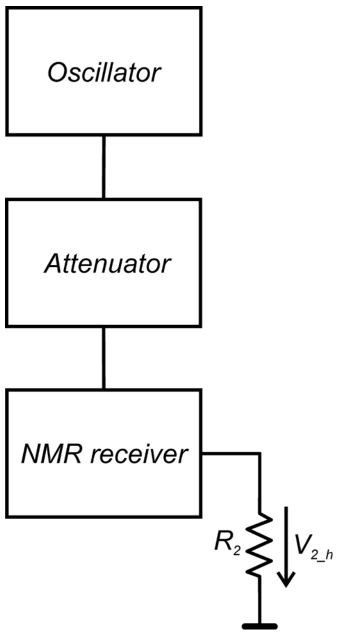

Fig.1. Simplified block diagram of the calibration with a harmonic oscillator.

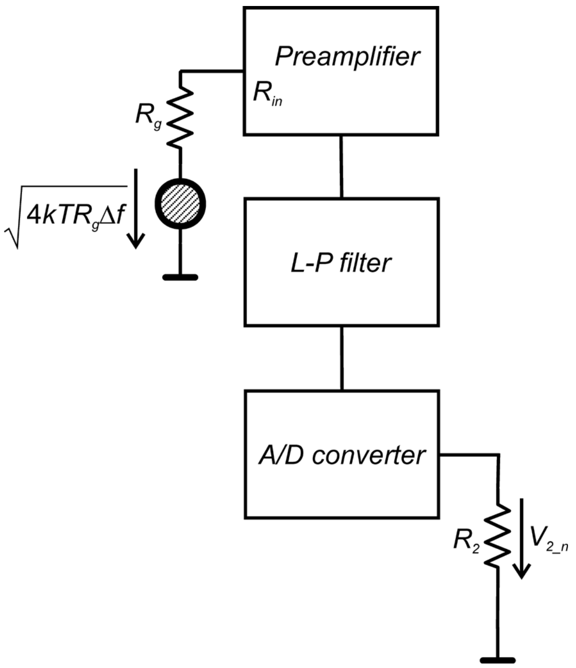

Fig.2. Simplified block diagram of the calibration with noise of a known resistance. The ADC is a part of the receiver.

The left side of (1) contains analogue quantities, the right side is an RMS voltage calculated from the series of frequency samples V_{2_n} measured by the receiver. V_{2_n} is given by (2)

$$V_{2\_n} = V_{2\_n\_1} \div V_{2\_n\_N} \tag{2}$$

The RMS voltage at the output of the receiver, corresponding to $R_{g\_50} = 50$ is given by (3)

$$V_{50} = V_{2\_n\ \_rms} = \sqrt{\left(\frac{1}{N}\right)^2 \cdot \sum_{i=n_1}^{n_2} \left|V_{2\_n\_i}\right|^2} \tag{3}$$

where $1 \leq n_1 < n_2 \leq N$. Spectrum between n_1 and n_2 should be considered constant. The noise bandwidth Δf must correspond to this limit. For calculation the calibration coefficient C in (1) must be measured two times with two different values of R_g. It is suitable if one of the R_g values is 0. Consider $R_g = R_{g\_50} = 50\ \Omega$. The measurement yields a system of two equations given by (4)

$$\begin{aligned} \sqrt{\left(\sqrt{4kTR_{g\_0}\Delta f}R_{in}/(R_{g\_0}+R_{in})C\right)^2 + V_{rec}^2} &= V_0 \\ \sqrt{\left(\sqrt{4kTR_{g\_50}\Delta f}R_{in}/(R_{g\_50}+R_{in})C\right)^2 + V_{rec}^2} &= V_{50} \end{aligned} \tag{4}$$

One of the possible solutions of (4) is (5), (6)

$$V_{rec} = V_0 \tag{5}$$

$$C = \frac{-\mathrm{i}(R_{g\_50}+R_{in})\sqrt{V_0^2 - V_{50}^2}}{2R_{in}\sqrt{d\Delta f k R_{g\_50} T}} \tag{6}$$

Where:
$\mathrm{i} = \sqrt{-1}$,
$d = n_2 - n_1$,
$\Delta f = \frac{d}{NT_s}$,
T_s is the sampling time interval.

It is obvious that the measurement can be done for different values of R_g without special requirements on instruments.

The processed data were measured under the following conditions:
operation frequency of the scanner: $f_0 = 4.45$ MHz
sampling interval: $T_s = 100$ µs
frequency bandwidth of the receiver: $B = 10$ kHz
temperature of R_g: $T = 296$ K
original number of samples: $N = 500{,}000$
number of samples after cropping: $d = 300{,}000$

3. RESULTS

Verification experiments were performed on an experimental NMR scanner equipped with a home-made resistive magnet of 0.1 T and the Apollo spectroscopic NMR console (Tecmag Inc., Houston, TX) was utilized for imaging, operated at a frequency of 4.45 MHz. Console calibration was performed using the GFG-3015 function generator (Good Will Instrument Co., Ltd., New Taipei City, Taiwan). The broadband preamplifier AU-1579 (MITEQ, Hauppauge, NY) with 50-Ohm input and output impedances and *NF* = 1 dB (a catalogue datum) was used. For calibration with harmonic signal (Experiment 1) the instruments were connected according to Fig.1. and the harmonic signal was set on the function generator. Magnitude of the 4.45 MHz signal was 5 mV. The signal from the generator proceeded into the attenuator of 60 dB. Magnitudes of the input and output signals have been compared and the ratio has been calculated. For calibration with noise of a known resistance (Experiment 2) the instruments have been connected according to Fig.2. RMS noise voltages V_0 and V_{50} have been measured and calculated for $R_g = 0\ \Omega$ and $R_g = 50\ \Omega$. The calibration coefficient has been calculated using (6). The results can be read in Table 1. It is obvious that using the technique, the receiver does not have to be matched; it means R_g may be different than 50 Ω. However, the experiments revealed that the value of *C* is a bit different for different R_g.

Table 1. Results of verification.

Experiment	f_0 [MHz]	Coefficient 1	Coefficient 2
1	4.45	4.96639×10^9	
2	4.45		5.17949×10^9

4. Discussion / conclusions

The purpose of this study was to test the techniques for the calibration of the NMR spectrometer receiver. The calibration has been carried out with two techniques and the results have been compared. The endeavor was to use only widely available or cheap instruments and materials. It was managed mainly with the second method using thermal noise of a known resistance. The calibrated NMR receiver can be utilized in several experiments. The calibration coefficient is the next feature of the NMR data. The first technique – with a signal generator – is advantageous mainly for matched components. The second technique – with noise of a known resistance – is suitable also for an unmatched receiver. Nevertheless, the calibration coefficient changes slightly with changing resistance. It can be a complication when applying the coefficient in an experiment and the ability of the unmatched operations may not be so significant. Not every receiver can be calibrated. Thus, proper console selection is also important. Difference between results of experiments 1 and 2 is approximately 4 %. Taking into account tolerances of the used devices, it is a good result.

Acknowledgment

This work was supported by the Scientific Grant Agency VEGA 2/0003/20, and within the project of the Research and Development Agency No. APVV-19-0032.

References

[1] Andris, P., Emery, E.F., Frollo, I. (2019). Analysis of NMR spectrometer receiver noise figure. *Mathematical Problems in Engineering,* 2019, 1083706. https://doi.org/10.1155/2019/1083706.

[2] Schiek, B., Siweris, H.J. (1990). *Rauschen in Hochfrequenzschaltungen [Noises in RF Circuits].* Hüthig, ISBN 978-3778520079. (in German)

[3] Žalud, V., Kulešov, V.N. (1980). *Polovodičové obvody s malým šumem [Semiconductor Circuits with Low Noise]*. Prague, Czech Republic: SNTL, ISBN 04-528-80. (in Czech)

[4] Hoult, D.I., Richards, R.E. (1976). The signal-to-noise ratio of the nuclear magnetic resonance experiment. *Journal of Magnetic Resonance*, 24 (1), 71-85. https://doi.org/10.1016/0022-2364(76)90233-X.

[5] Hoult, D.I., Lauterbur, P.C. (1979). The sensitivity of the zeugmatographic experiment involving human samples. *Journal of Magnetic Resonance*, 34 (2), 425-433. https://doi.org/10.1016/0022-2364(79)90019-2.

[6] Raad, A., Darrasse, L. (1992). Optimization of NMR bandwidth by inductive coupling. *Magnetic Resonance Imaging*, 10 (1), 55-65. https://doi.org/10.1016/0730-725x(92)90373-8.

[7] Décorps, M., Blondet, P., Reutenauer, H., Albrand, J.P., Remy, C. (1985). An inductively coupled, series-tuned NMR probe. *Journal of Magnetic Resonance*, 65 (1), 100-109. https://doi.org/10.1016/0022-2364(85)90378-6.

[8] Vergara, Gomez, T.S., Dubois, M., Glybovski, S., Larrat, B., De Rosny, J., Rockstuhl, C., Bernard, M., Abdeddaim, R., Enoch, S., Kober, F. (2019). Wireless coils based on resonant and nonresonant coupled-wire structure for small animal multinuclear imaging. *NMR in Biomedicine*, 32 (5), e4079. https://doi.org/10.1002/nbm.4079.

[9] Qian, Ch., Duan, Q., Dodd, S., Koretsky, A., Murphy-Boesch, J. (2016). Sensitivity enhancement of an inductively coupled local detector using a HEMT-based current amplifier. *Magnetic Resonance in Medicine*, 75 (6), 2573-2578. https://doi.org/10.1002/mrm.25850.

[10] Weis, J., Ericsson, A., Hemmingsson, A. (1999). Chemical shift artifact-free microscopy: Spectroscopic microimaging of the human skin. *Magnetic Resonance in Medicine*, 41 (5), 904-908. https://doi.org/10.1002/(SICI)1522-2594(199905)41:5%3C904::AID-MRM8%3E3.0.CO;2-4.

[11] Marcon, P., Bartusek, K., Dokoupil, Z., Gescheidtova, E. (2012). Diffusion MRI: Mitigation of magnetic field inhomogeneities. *Measurement Science Review*, 12 (5), 205-212. https://sciendo.com/de/article/10.2478/v10048-012-0031-8.

[12] Bartusek, K., Dokoupil, Z., Gescheidtova, E. (2007). Mapping of magnetic field around small coil using the magnetic resonance method. *Measurement Science and Technology*, 18 (7), 2223-2230. https://doi.org/10.1088/0957-0233/18/7/056.

[13] Nespor, D., Bartusek, K., Dokoupil, Z. (2014). Comparing saddle, slotted-tube and parallel-plate coils for Magnetic Resonance Imaging. *Measurement Science Review*, 14 (3), 171-176. https://doi.org/10.2478/msr-2014-0023.

[14] Latta, P., Gruwel, M.L., Volotovskyy, V., Weber, M.H., Tomanek, B. (2007). Simple phase method for measurement of magnetic field gradient waveforms. *Magnetic Resonance Imaging*, 25 (9), 1272-1276. https://doi.org/10.1016/j.mri.2007.02.002.

[15] Latta, P., Gruwel, M.L., Volotovskyy, V., Weber, M.H., Tomanek, B. (2008). Single-point imaging with a variable phase encoding interval. *Magnetic Resonance Imaging*, 26 (1), 109-116. https://doi.org/10.1016/j.mri.2007.05.004.

[16] Wimmer, G., Witkovský, V., Duby, T. (2000). Proper rounding of the measurement results under normality assumptions. *Measurement Science and Technology*, 11 (12), 1659-1665. https://doi.org/10.1088/0957-0233/11/12/302.

[17] Witkovsky, V., Frollo, I. (2020). Measurement science is the science of sciences - there is no science without measurement. *Measurement Science Review*, 20 (1), 1-5. https://doi.org/10.2478/msr-2020-0001.

Received August 15, 2021
Accepted October 14, 2021